

# Involvement of *Escherichia coli* YbeX/CorC in ribosomal metabolism

İsmail Sarigül<sup>1</sup>, Amata Žukova<sup>1</sup>, Emel Alparslan<sup>1</sup>, Sille Remm<sup>1</sup>, Margus Pihlak<sup>2</sup>, Niilo Kaldalu<sup>1</sup>, Tanel Tenson<sup>1</sup>, and Ülo Maiväli<sup>1</sup>

<sup>1</sup>Tartu Ülikooli Tehnoloogiasinstituut

<sup>2</sup>Tallinna Tehnikaulikool Küberneetika instituut

October 28, 2023

## Abstract

YbeX of *Escherichia coli*, a member of the CorC protein family, is encoded in the same operon with ribosome-associated proteins YbeY and YbeZ. Here, we report the involvement of YbeX in ribosomal metabolism. The  $\Delta\psi\beta\epsilon\Xi$  cells accumulate distinct 16S rRNA degradation intermediates in the 30S particles and the 70S ribosomes. *E. coli* lacking *ybeX* has a lengthened lag phase upon outgrowth from the stationary phase. This growth phenotype is heterogeneous at the individual cell level and especially prominent under low extracellular magnesium levels. The  $\Delta\psi\beta\epsilon\Xi$  strain is sensitive to elevated growth temperatures and to several ribosome-targeting antibiotics that have in common the ability to induce the cold shock response in *E. coli*. Although generally milder, the phenotypes of the  $\Delta\psi\beta\epsilon\Xi$  mutant overlap with those caused by *ybeY* deletion. A genetic screen revealed partial compensation of the  $\Delta\psi\beta\epsilon\Xi$  growth phenotype by the overexpression of YbeY. These findings indicate an interconnectedness amongst the *ybeZYX* operon genes, highlighting their roles in ribosomal assembly and/or degradation.

## INTRODUCTION

Ribosome biogenesis is a highly regulated process encompassing concomitant transcription, processing, degradation, modification, and folding of ribosomal RNAs, equimolar synthesis, and incorporation into ribosomes of more than 50 different ribosomal proteins (Davis and Williamson, 2017). In bacteria, this is catalyzed, chaperoned, and generally facilitated by dozens of dedicated proteins working in several partially overlapping and redundant pathways (Shajani *et al.*, 2011). However, due to its sheer complexity, our understanding of this process relies on isolated fragments of processing/folding pathways, with minimal knowledge of many individual factors' precise mechanisms of action.

It has long been known that  $Mg^{2+}$  is necessary for ribosomal assembly and translation (McCarthy *et al.*, 1962). More recently, it was discovered that intracellular free  $Mg^{2+}$  concentrations and rRNA transcription rates are actively co-regulated for achieving optimal ribosomal assembly and translation (Pontes *et al.*, 2016). Also,  $Mg^{2+}$  influx can alleviate ribosomal stress phenotypes, probably by stabilizing the ribosomal structure (Lee *et al.*, 2019). *ybeX* encodes a putative  $Co^{2+}/Mg^{2+}$  efflux protein, which, while highly conserved in bacteria, is poorly characterized (Kazakov *et al.*, 2003; Anantharaman and Aravind, 2003). The *ybeX/corC* gene was initially discovered in *Salmonella enterica* serovar Typhimurium in a screen for cobalt resistance and was proposed to contribute, possibly as a co-effector of the metal transport protein CorA, to the efflux of divalent cations (Gibson *et al.*, 1991). Notwithstanding over 97% sequence similarity between *E. coli* and *Salmonella ybeX/corC*, a corresponding study in *E. coli* is absent. The levels of YbeX (but not YbeY and YbeZ) mRNA and protein are about two-fold reduced under low-magnesium conditions (Caglar *et al.*, 2017). Intriguingly, as a serendipitous finding, *E. coli* cells that rely for growth on an artificial ribosome variant, where fused rRNAs covalently tether the subunits, have increased growth rate caused by a nonsense

mutation in the *ybeX* gene together with a missense mutation in the ribosomal protein gene *rpsA* (Orelle *et al.* , 2015).

In the *E. coli* genome, *ybeX* is located in the *ybeZYX-Int* operon (**Fig. 1A**), transcripts of which have not been fully mapped. The *lnt* gene, which encodes an essential inner membrane protein, is predicted to be under the control of the minor heat shock sigma factor  $\sigma^{24}$  (RpoE) (Keseler *et al.* , 2013), while transcription of *ybeZ*, *ybeY*, *ybeX* and *lnt* is regulated by the primary heat shock sigma factor  $\sigma^{32}$  (RpoH) (Nonaka *et al.* , 2006).

The most-studied member of the *ybeZYX-lnt* operon is *ybeY*, whose importance in ribosomal metabolism is beyond dispute, while its precise mode of action remains unclear (Davies *et al.* , 2010). The YbeY is, by sequence homology and structural studies, a zinc-dependent RNA endonuclease. It is extremely highly conserved, has strong, albeit heterogeneous phenotypes in every organism that has been looked into, and is required to correctly process the 3' end of 16S rRNA (Liao *et al.* , 2021). Moreover, *ybeY* mutants have been shown to be defective in translation and to accumulate defective ribosomes in several bacterial species, mitochondria and chloroplasts (Liu *et al.* , 2015; Liao *et al.* , 2021; D'Souza *et al.* , 2021). And yet, in the purified form, its RNase activity seems to be limited to short RNA oligonucleotides (Jacob *et al.* , 2013; Babu *et al.* , 2020), while *in vitro* processing of the 16S rRNA 3'-end can be achieved without it (Smith *et al.* , 2018).

The *ybeZ* gene is located upstream of *ybeY*, having four nucleotides overlap. *ybeZ* encodes a phosphate starvation-regulated PhoH subfamily protein with the NTP hydrolase domain (Kim *et al.* , 1993). YbeZ has phosphatase activity and is a putative RNA helicase through sequence homology (Kazakov *et al.* , 2003; Andrews and Patrick, 2022). A physical interaction between YbeY and YbeZ was suggested based on bacterial two-hybrid system experiments in *E. coli* (Vercruyssen *et al.* , 2016). Their interaction has been biochemically verified in *Pseudomonas aeruginosa* (Xia *et al.* , 2020). In an *E. coli* interactome study, it has been observed that YbeZ not only interacts with YbeY but also exhibits interactions with numerous ribosomal proteins (Butland *et al.* , 2005).

In this work, we investigate the effects of *ybeX* deletion on *E. coli* growth and ribosomal metabolism.

## RESULTS

### *Deletion of ybeX leads to heat sensitivity and longer outgrowth from the stationary phase*

*ybeX* belongs to the RpoH heat response regulon (Nonaka *et al.* , 2006). We tested by a spot assay the effect of elevated growth temperature on the  $\Delta\psi\beta\epsilon\Xi$  strain from the Keio collection (Baba *et al.* , 2006), compared to the isogenic wild-type strain. After overnight growth in the LB liquid medium, serial dilutions of the cultures were spotted on LB agar plates and incubated at 20°C, 37°C or 42°C overnight. Disruption of the *ybeX* gene hindered growth at 42°C but not at 20°C (**Fig. 1B**, **Fig. S1a**). For verification, *ybeX* deletion was reintroduced in two strain backgrounds, MG1655 and BW25113 (see **Fig. S1b, c** for strain construction). Heat sensitivity was retained in newly constructed  $\Delta\psi\beta\epsilon\Xi$  strains (**Fig. S1d**), demonstrating that the observed phenotype is *ybeX*-inflicted. We used the *ybeX* deletion strain of the Keio collection in further experiments.

Next, we assessed whether the lack of the YbeX protein caused the heat sensitivity, as secondary effects of the chromosomal deletion could be responsible for the phenotype. We reintroduced *ybeX* on a single-copy TransBac library plasmid (Otsuka *et al.* , 2015) and found that the leaky expression of YbeX in the absence of the inducer (isopropyl- $\beta$ -D-1-thiogalactopyranoside; IPTG) is sufficient to rescue the heat sensitivity phenotype of the  $\Delta\psi\beta\epsilon\Xi$  mutant. The empty vector and TransBac plasmids carrying *ybeY* or *ybeZ* had no effect on growth (**Fig. 1B**). Thus, the heat sensitivity of the  $\Delta\psi\beta\epsilon\Xi$  strain is caused by the absence of the YbeX protein rather than through polar effects on neighbouring genes.

To find which growth phase is affected by the *ybeX* deletion, we monitored bacterial growth in liquid LB medium at 37°C in 96-well plates. We did not notice differential growth of WT and  $\Delta\psi\beta\epsilon\Xi$  strains when cultures were started from freshly grown single colonies (data not shown). In contrast, when cultures were

inoculated with bacteria from the stationary phase overnight cultures, the  $\Delta\psi\beta\epsilon\Xi$  mutant had a much longer lag phase (300-350 min.) than the WT (100-150 min.; **Fig. 1C** , **Fig. S2a** ). Both strains reached similar optical densities in the stationary phase. A similar number of colonies of WT and  $\Delta\psi\beta\epsilon\Xi$  strains (**Fig. 1B** ) indicates that the delay of the visible growth of the  $\Delta\psi\beta\epsilon\Xi$  mutant is not caused by decreased survival in the stationary phase. The expression of *ybeX* from a single-copy TransBac library plasmid completely complemented the prolonged lag phase. In contrast, complementation with plasmids carrying *ybeY* , *ybeZ* or *lnt* had no effect, confirming that lack of the YbeX protein is causing the delay of regrowth while again excluding polar effect as the cause of the  $\Delta\psi\beta\epsilon\Xi$  phenotype (**Fig. 1C**; **Fig. S2b** ).

To investigate whether the longer lag phase of the  $\Delta\psi\beta\epsilon\Xi$  strain is due to lower metabolic activity in the mutant cells, we used the Alamar Blue reagent, a quantitative indicator of the oxidation-reduction potential of cell membranes, as a proxy for metabolic activity (Rampersad, 2012). In a control experiment conducted in PBS buffer lacking the nutrients necessary for the resumption of growth, both strains show similarly low Alamar Blue signal, indicating similar levels of metabolic activity (the superimposed black lines in **Fig. S2c** ). When cells were diluted into fresh LB medium, the Alamar Blue fluorescence immediately started to increase for both strains, indicating similar levels of cellular metabolism (**Fig. S2d, e** ). While the initial rate of increase in the Alamar Blue fluorescence is indistinguishable in WT and  $\Delta\psi\beta\epsilon\Xi$  cells, the WT acquires a faster rate of metabolism after about 100 minutes, while the  $\Delta\psi\beta\epsilon\Xi$  cells continue as before for about 200 more minutes (**Fig. S2d** ). As shown by the OD<sub>600</sub> measurements (**Fig. S2a** ), for both the WT and the  $\Delta\psi\beta\epsilon\Xi$  cells, the increase in fluorescence is accompanied by the start of regrowth (**Fig. S2e** ). These results indicate that the extended lag phase of the  $\Delta\psi\beta\epsilon\Xi$  strain is not caused by lower levels of metabolic activity upon transfer from the stationary phase culture into the regrowth medium.

*Τηε δελαψεδ ουτγρωωτη οφ τηε ΔψβεΞ μυταντ ις ηετερογενεουσ ατ τηε ινδιιδυαλ σελλ λεελ*

When streaking out mutant strains from glycerol stocks and overnight grown stationary phase cultures, we noticed that the  $\Delta\psi\beta\epsilon\Xi$  strain produces colonies of different sizes. Re-streaking of small and large  $\Delta\psi\beta\epsilon\Xi$  colonies resulted in similarly-sized second-generation colonies, indicating that the heterogeneous phenotype is not caused by a genetic mutation (data not shown). We hypothesized that the colony size heterogeneity of  $\Delta\psi\beta\epsilon\Xi$  is a result of the delayed outgrowth of individual bacteria and indicates physiological heterogeneity of the stationary phase inoculum.

Inspection of colony sizes plated from overnight grown bacterial cultures showed, in agreement with our previous observations, that  $\Delta\psi\beta\epsilon\Xi$  cells tend to form smaller colonies than wild-type (WT) cells when grown overnight in LB or MOPS minimal medium supplemented with 0.3% glucose (**Fig. 2A** , **Fig. S3a** ). To better understand the nature of the  $\Delta\psi\beta\epsilon\Xi$  phenotype at the individual cell level, colony radiuses of  $\Delta\psi\beta\epsilon\Xi$  and WT were quantified from four independent stationary phase outgrowth experiments using AutocellSeg (Khan *et al.* , 2018). Overnight-grown cells were plated from LB or MOPS minimal media, and plates were incubated at 37°C or 42°C overnight. When plated from the LB medium,  $\Delta\psi\beta\epsilon\Xi$  cells formed smaller and more heterogeneous colonies than wild-type cells (**Fig. 2A** , **B** ). In contrast, when plated from the MOPS minimal medium, the  $\Delta\psi\beta\epsilon\Xi$  colonies appear to be consistently smaller and more homogeneous in size (**Fig. 2C** ). We found that a fraction of  $\Delta\psi\beta\epsilon\Xi$  cells lost the ability of colony formation when plates were incubated at 42°C (**Fig. 2D** ). When plated from LB, this drop was about 10-fold ( $p < 0.0001$ ) and from MOPS medium about two-fold ( $p=0.055$ , **Fig. 2D** ). Nonetheless, the quantified colony radiuses on plates incubated at 42°C resembled those at 37°C (**Fig. 2B** , **C** ).

While the  $\Delta\psi\beta\epsilon\Xi$  colony sizes were increased after 48 hours of incubation at 37°C, they consistently remained heterogeneous in size in the absence or presence of the kanamycin resistance cassette (**Fig. S3b** , **c** ). In conclusion, the  $\Delta\psi\beta\epsilon\Xi$  cells grow in at least two distinct regimes, one similar to WT growth, while the other results in up to two-fold smaller colonies.

*Τηε ΔψβεΞ στραιν ις σενοιτιε το ριβσοομε-ταργετινγ αντιβιοτιςς*

*ybeX* disruption has been reported to cause decreased survival in the presence of chloramphenicol (Smith *et al.* , 2007). Therefore, we explored the effects of various antibiotics on the  $\Delta\psi\beta\epsilon\Xi$  cells. First, we

determined the minimal inhibitory concentrations (MICs) in LB for *WT* and  $\Delta\psi\beta\epsilon\Xi$  strains. The MICs of chloramphenicol, tetracycline, erythromycin, clindamycin, and fusidic acid were two times lower for  $\Delta\psi\beta\epsilon\Xi$  (**Table S1**). These structurally unrelated ribosome-targeting antibiotics have been shown to induce cold-shock proteins or block the induction of heat-shock proteins (VanBogelen and Neidhardt, 1990; Cruz-Loya *et al.*, 2019).

We further inspected the effects of these antibiotics using the dot spot assay described above, except that the LB agar plates were supplemented with sub-MIC concentrations of indicated antibiotics (see Materials and Methods). The  $\Delta\psi\beta\epsilon\Xi$  strain exhibited severe sensitivity to sub-MIC concentrations of chloramphenicol, tetracycline, erythromycin, clindamycin, and fusidic acid (**Fig. 3A**). The presence of *ybeX* single-copy plasmid in the absence of inducer fully rescued the described antibiotic sensitivities (**Fig. 3B**). In contrast, protein synthesis-targeting antibiotics that do not induce the cold shock response (amikacin, streptomycin, kanamycin, tobramycin and mupirocin), exhibit similar inhibitory effect on  $\Delta\psi\beta\epsilon\Xi$  and *WT* strains. The RNA synthesis inhibitor rifampicin also revealed no differential effect on the  $\Delta\psi\beta\epsilon\Xi$  strain (**Fig. 3B, Fig. S4b**).

To exclude strain-specific effects, we tested two isogenic wild-type strains, MG1655 and BW25113 and the corresponding deletion strains  $\Delta\psi\beta\epsilon\Xi::\kappa av^{MT}$  and  $\Delta\psi\beta\epsilon\Xi::\kappa av^{B\Omega}$  under sub-inhibitory antibiotic concentrations (**Fig. S4b**). Both genetic backgrounds exhibited similar antibiotic sensitivities, and removal of the kanamycin resistance cassette (in strains  $\Delta\psi\beta\epsilon\Xi/-\kappa av^{MT}$  and  $\Delta\psi\beta\epsilon\Xi/-\kappa av^{B\Omega}$ ) had no effect.

*Τηρ δελαιψεδ ουτγρωωτη ανδ αντιβιοτις σενοσιτιψ οφ ΔψβεΞ δεπεινδ ον τηρ γρωωτη ηιστοριψ οφ βακτηρια*

While the  $\Delta\psi\beta\epsilon\Xi$  cells have a lengthened lag phase during outgrowth from the stationary phase, they appear to retain similar levels of metabolic activity to the *WT* cells during this lag phase, as well as similar exponential growth rate (**Fig. 1D**). This led us to hypothesize that any cellular defects conferred by the lack of *YbeX* could accumulate stochastically during late growth, preceding entry into the stationary phase and/or in the stationary phase itself, which in turn could lead to the observed single-cell heterogeneity during outgrowth (**Fig. 2**). Accordingly, we tested whether the phenotypes of  $\Delta\psi\beta\epsilon Z$ ,  $\Delta\psi\beta\epsilon\Psi$ , and  $\Delta\psi\beta\epsilon\Xi$  depend on the growth phase of the culture from where the cells originate. We surmised that if a gradual accumulation of harm causes the  $\Delta\psi\beta\epsilon\Xi$  phenotype, then cells that have had more time to accumulate such harm should exhibit stronger phenotypes.

Overnight-grown cultures of  $\Delta\psi\beta\epsilon Z$ ,  $\Delta\psi\beta\epsilon\Psi$ ,  $\Delta\psi\beta\epsilon\Xi$  and wild-type (*WT*) strains were serially diluted and spotted on LB agar plates to assay the heat and antibiotic sensitivity. The same stationary phase cultures were diluted a hundred-fold into fresh LB medium and then grown at 37°C for four to five cell divisions until  $OD_{600}$  reached 0.2-0.4, after which the cells were diluted and spotted on LB agar plates to assay the heat and antibiotic sensitivity of exponentially growing cells.

The  $\Delta\psi\beta\epsilon\Xi$  stationary phase inoculum exhibited sensitivity to sub-MIC concentrations of chloramphenicol and erythromycin but no sensitivity to rifampicin in comparison to *WT* (**Fig. 4A**). In contrast, the exponentially growing  $\Delta\psi\beta\epsilon\Xi$  had *WT*-like sensitivity to all tested antibiotics. In comparison,  $\Delta\psi\beta\epsilon Z$  cultures had intermediate levels of sensitivity to chloramphenicol, regardless of the growth history of cells, while they are not more sensitive to erythromycin, rifampicin, and tetracycline as compared to *WT* (**Fig. 4A**). Exponentially growing  $\Delta\psi\beta\epsilon Z$  cells in MOPS minimal medium, supplemented with 0.3% glucose, also exhibited sensitivity to chloramphenicol (**Fig. S4a**).  $\Delta\psi\beta\epsilon\Psi$  cells were very sensitive to all tested antibiotics, notwithstanding the growth phase of the spotted culture.

In liquid media, cultures started directly from stationary phase inocula again showed a lengthened lag phase for  $\Delta\psi\beta\epsilon\Xi$  but not for  $\Delta\psi\beta\epsilon Z$ , while the exponential growth rates of both  $\Delta\psi\beta\epsilon\Xi$  and  $\Delta\psi\beta\epsilon Z$  were very similar to *WT* (**Fig. 4B**). The  $\Delta\psi\beta\epsilon\Psi$  strain behaves similarly, regardless of the growth phase of inoculums, exhibiting a reduced exponential growth rate and reaching a lower maximal cell density. In contrast, when the cells were outgrown from exponential phase cultures, the *WT*,  $\Delta\psi\beta\epsilon Z$  and  $\Delta\psi\beta\epsilon\Xi$  strains grew equally well, with no visible lag phase, while the  $\Delta\psi\beta\epsilon\Psi$  strain had a reduced growth rate and a lower growth end-point, as expected (**Fig. 4C**).

Τηρ  $\Delta\psi\beta\epsilon\Xi$  ζελλς αςσυμυλατε ρΡΝΑ φραγμαεντς

As *ybeX* is located in the same operon with *ybeY*, which is implicated in ribosome assembly, we assessed the rRNA profiles of total cellular RNA of the WT and the  $\Delta\psi\beta\epsilon Z$ ,  $\Delta\psi\beta\epsilon\Psi$ , and  $\Delta\psi\beta\epsilon\Xi$  strains by Northern blotting. For membrane hybridization, we used probes specific for the 17S precursor rRNA, the mature 16S rRNA and the 23S rRNA (**Fig. 5A**).

In exponentially growing  $\Delta\psi\beta\epsilon\Psi$  cells, we saw a substantial accumulation of immature 17S rRNA, while  $\Delta\psi\beta\epsilon\Xi$  and  $\Delta\psi\beta\epsilon Z$  cells had comparable levels of 17S rRNA to wild-type (**Fig. 5B, D, E**).  $\Delta\psi\beta\epsilon\Psi$  cells also accumulate a faster-migrating 16S rRNA species, labelled as 16S\* (**Fig. 5B**; see also (Davies *et al.*, 2010)). The  $\Delta\psi\beta\epsilon\Xi$  lysates do not contain the 16S\* rRNA species.

When we assessed the total RNA extracted from stationary phase  $\Delta\psi\beta\epsilon\Xi$  cell cultures, we observed an accumulation of 16S and 23S rRNA fragments (**Fig. 5B, C**). These fragments were not present in material obtained from exponentially grown  $\Delta\psi\beta\epsilon\Xi$  cells. Wild type,  $\Delta\psi\beta\epsilon Z$  and  $\Delta\psi\beta\epsilon\Psi$  cells exhibited no such fragments in stationary or exponentially growing cells. Both  $\Delta\psi\beta\epsilon\Xi$  and  $\Delta\psi\beta\epsilon\Psi$  stationary cells accumulate 17S rRNA (**Fig. 5D, E**).

In addition, the stationary phase  $\Delta\psi\beta\epsilon\Xi$  cells accumulate a wide spectrum of 17S pre-rRNA degradation intermediates ranging from a couple of hundred nucleotides to almost full-length 16S rRNA, as detected by the 17S 5'-end specific oligonucleotide (**Fig. 5D**). **Fig. 5E**, where we use a 3'-end specific oligonucleotide, indicates that these decay intermediates lack the 17S 3'-end. WT,  $\Delta\psi\beta\epsilon Z$  and  $\Delta\psi\beta\epsilon\Psi$  lysates lack such degradation intermediates. Thus, the  $\Delta\psi\beta\epsilon\Xi$  cells have a unique and disparate mixture of 17S rRNA and 16S rRNA degradation intermediates.

Τηρ  $\Delta\psi\beta\epsilon\Xi$  στραιν αςσυμυλατες διστινστ ρΡΝΑ σπεςιες αλρεαδψ δυρινγ τηρ λατε εξπονεντιαλ γρωωτη

As there is neither substantial assembly nor degradation of mature ribosomes in the stationary phase (Pirr *et al.*, 2011), we conjectured that the accumulated fragments observed in  $\Delta\psi\beta\epsilon\Xi$  cells were likely getting there by the late exponential phase. Accordingly, we purified ribosomal subunits from late exponential cells by sucrose gradient fractionation and assayed the rRNA composition of the 70S ribosomes, 50S and 30S ribosomal subunits by Northern blotting.

The sucrose gradient profiles for wild-type (WT) and  $\Delta\psi\beta\epsilon\Xi$  lysates are very similar, with the vast majority of ribosomal particles being in the 70S ribosome fraction and the relatively minor free subunit fractions exhibiting no apparent abnormalities (**Fig. 6A**). Northern blots revealed full-length 17S pre-rRNA in the 30S fractions of both the WT and the  $\Delta\psi\beta\epsilon\Xi$  strains, as detected via 16S and 17S rRNA specific oligonucleotides (**Fig. 6B -E**). In the  $\Delta\psi\beta\epsilon\Xi$  strain, the mature 16S rRNA is substantially reduced in the 30S fraction compared to the WT (**Fig. 6B, C**). Thus, in the  $\Delta\psi\beta\epsilon\Xi$  cells, the 30S (SSU) fraction was unlikely to contain many functionally active small ribosomal subunits.

In addition,  $\Delta\psi\beta\epsilon\Xi$  cells accumulated distinct truncated 16S rRNA and 17S pre-rRNA fragments, missing the 3'-end or 5'-end, in the ribosomal fractions (**Fig. 6B -E**, denoted as “trunc.”). Firstly, a 5'-end truncated 16S rRNA fragment is present in all ribosomal fractions of the  $\Delta\psi\beta\epsilon\Xi$  strain, including the 70S ribosomes, as detected via 16S rRNA and 16S 3'-end specific oligonucleotides (**Fig. 6B, C**). Secondly, truncated 17S rRNA fragments were present only in the 30S fraction of  $\Delta\psi\beta\epsilon\Xi$ , as detected via 17S 5' and 3' ends rRNA-specific probes (**Fig. 6D, E**). Truncated 17S pre-rRNA fragments, presumably arising from the precursor SSU particles, are absent in the 70S and 50S fractions (**Fig. 6D, E**). Decay intermediates in the 30S fraction indicate that most pre-SSU particles are inactive and degradation-bound in late-exponential phase  $\Delta\psi\beta\epsilon\Xi$  cultures. In contrast, the 23S rRNA specific probe reveals only relatively minor differences in degradation patterns between WT and  $\Delta\psi\beta\epsilon\Xi$  strains (**Fig. 6F**).

We tested the effect of chloramphenicol (CAM), a well-studied protein synthesis inhibitor (Wilson, 2014), treatment on the ribosomes by sucrose gradient fractionation and northern blotting (**Fig. S5a**). The sucrose gradient profiles of the WT and  $\Delta\psi\beta\epsilon\Xi$  strain lysates were similar, while CAM-treated ribosomal particles sedimented notably differently from those of mature subunits (**Fig. S5b**; see also (Siibak *et al.*, 2009)).

However, in the  $\Delta\psi\beta\epsilon\Xi$  strain, in Northern blots, we observed distinct aberrant 16S rRNA fragments, which were absent in the WT (**Fig. S5c**). In addition, the CAM treatment, which leads to bacterial growth arrest, stabilizes the  $\Delta\psi\beta\epsilon\Xi$  30S particles. While CAM 30S particles contain a good measure of 16S rRNA and 17S pre-rRNA in the  $\Delta\psi\beta\epsilon\Xi$  strain, the  $\Delta\psi\beta\epsilon\Xi$  30S particles from the control experiment without CAM treatment contain fragments of SSU rRNA and reduced amounts of mature SSU rRNA (**Fig. S5c**). These findings indicate that the accumulation of decay intermediates in  $\Delta\psi\beta\epsilon\Xi$  is not an artefact that occurs during the purification of ribosomal samples but occurs *in vivo*. This interpretation is further supported by the fact that hot phenol-extracted total RNA samples harbour similar fragments of rRNA (**Fig. 5**).

These results indicate that in the late exponential phase, RNA in most of the free 30S subunits of the  $\Delta\psi\beta\epsilon\Xi$  strain is being fragmented. Moreover, the degradation fragments captured by the 16S rRNA and 17S rRNA-specific probes strongly suggest that in the  $\Delta\psi\beta\epsilon\Xi$  strain, pre-ribosomes (in the 30S fraction) and mature ribosomes (in the 70S fraction) are susceptible to degradation.

*Τηρ  $\Delta\psi\beta\epsilon\Xi$  μταντ πηνουτπες ζαν βε ουππρεσοεδ βψ Μγ<sup>2+</sup> ουππλεμενταιον*

As YbeX has been implicated in Mg<sup>2+</sup> efflux (Gibson *et al.*, 1991), we tested whether supplementing growth media with magnesium chloride affects the  $\Delta\psi\beta\epsilon\Xi$ -caused phenotypes. First, we grew the WT and  $\Delta\psi\beta\epsilon\Xi$  strains in LB medium with and without magnesium supplementation (**Fig. 7A, Fig. S6a**). When bacteria were grown in LB medium that was supplemented with 10 mM MgCl<sub>2</sub>, the antibiotic and heat sensitivity of  $\Delta\psi\beta\epsilon\Xi$  mutant upon plating disappeared (**Fig. 7A**). To test whether the effect of Mg<sup>2+</sup> is media-dependent, we used the SOB medium, which contains 10 mM MgCl<sub>2</sub>. Again, the phenotypes of  $\Delta\psi\beta\epsilon\Xi$  disappeared. Thus, excess magnesium in the growth media, either LB or SOB, fully rescued the growth and ribosomal phenotypes of the  $\Delta\psi\beta\epsilon\Xi$  cells (**Fig. S6a, b**).

To test whether magnesium-deficient-rich media could increase the severity of the growth phenotype, we used the peptide-based medium (PBM), a rich, magnesium-limited, buffered, complex growth medium (Christensen *et al.*, 2017) that is free of any cell extract, which is the primary source of magnesium in almost all complex media (Liet *et al.*, 2020). We modified it to contain casamino acids instead of glucose to avoid diauxic inhibition.  $\Delta\psi\beta\epsilon\Xi$  cells had longer lag times during outgrowth in PBM than in LB (**Fig. S6c**), while wild-type cells grown in LB or PBM did not differ in outgrowth. The heat sensitivity upon plating was more severe in PBM than in LB medium (**Fig. 7B, Fig. S6d, e**). Supplementation of PBM with 50 μM and 100 μM MgCl<sub>2</sub> partially suppressed and 200 μM MgCl<sub>2</sub> completely suppressed the outgrowth delay of  $\Delta\psi\beta\epsilon\Xi$  at 37°C and 42°C (**Fig. 7B**). Supplementation of LB with 100 mM MgCl<sub>2</sub> completely suppressed the outgrowth delay of  $\Delta\psi\beta\epsilon\Xi$ , with no impact on the growth rates of wild-type and  $\Delta\psi\beta\epsilon\Xi$  strains (**Fig. S7a**).

We further tested the Mg<sup>2+</sup>-sensitivity of the  $\Delta\psi\beta\epsilon\Xi$  mutant in the MOPS minimal medium supplemented with 0.5% glucose. Unlike in PBM, we can precisely control the magnesium levels in the MOPS medium (Neidhardt *et al.*, 1974). The  $\Delta\psi\beta\epsilon\Xi$  cultures achieved similar optical density plateaus to the wild-type. This holds for a wide range of Mg<sup>2+</sup> concentrations in the MOPS minimal medium (**Fig. S7b**). When WT cells were grown into stationary phase in the MOPS minimal medium, the Mg<sup>2+</sup> concentration had no effect on the time-to-outgrowth (**Fig. 7C**, the left panel). Neither was there any effect on the growth rates. Under matching conditions, the  $\Delta\psi\beta\epsilon\Xi$  strain grown in [?]<sub>50</sub> μM Mg<sup>2+</sup> exhibited extended lag phases of 350 to 400 minutes. The presence of [?]<sub>75</sub> μM MgCl<sub>2</sub> decreases the lag time to about 200 minutes, after which additional magnesium has little effect on the duration of the lag phase (**Fig. 7C**, the right panel). These results indicate that the effects of *ybeX* deletion can be compensated by elevated Mg<sup>2+</sup> concentration of the growth medium.

*ΔψβεΞ πηνουτπες αρε προμινεντ υνδερ λωω εξτρασελλυλαρ μαγνεσιυμ ανδ δυρινγ τηρ τρανσιτιον ιντο τηρ στατιοναριψ πηασε*

Our ability to control the  $\Delta\psi\beta\epsilon\Xi$  phenotype by Mg<sup>2+</sup> allowed us to pinpoint the growth phase dependence of the  $\Delta\psi\beta\epsilon\Xi$  phenotype more precisely. Therefore, in the next experiment, we first grew the cultures overnight into the stationary phase in MOPS minimal medium supplemented with 10 mM MgCl<sub>2</sub> and 0.5% glucose,

where  $\Delta\psi\beta\epsilon\Xi$  phenotype does not occur. Then, the cells were washed thrice with MOPS minimal medium lacking  $Mg^{2+}$ , after which the regrowth assay was set up by suspending the cells in MOPS containing 10  $\mu M$   $MgCl_2$  (**Fig. 8A**).

As expected, there is no difference in the duration of the outgrowth lag phase between the wild-type and  $\Delta\psi\beta\epsilon\Xi$ , and the exponential growth rates were the same (**Fig. 8B**). To look for the emerging  $\Delta\psi\beta\epsilon\Xi$  phenotype, we plated spots of samples from the outgrowth cultures at designated time points (**Fig. 8B**) onto both LB and R2A agar plates (R2A stimulates the growth of stressed bacteria). The plates were incubated overnight at 37°C or 42°C. While until the 4h time point there was no difference between the colony formation of WT and  $\Delta\psi\beta\epsilon\Xi$  (**Fig. 8C**), upon transition into the stationary phase, in the 5.5h time point, there is a growth delay of the  $\Delta\psi\beta\epsilon\Xi$  strain on both LB or R2A agar plates, which is more pronounced at 42°C. Similarly, the sensitivity of the  $\Delta\psi\beta\epsilon\Xi$  strain to tetracycline, erythromycin and chloramphenicol antibiotics appears only at the 5.5h time point (**Fig. 8D**). We conclude that the delay of regrowth and antibiotic sensitivity of the  $\Delta\psi\beta\epsilon\Xi$  strain appears under low extracellular magnesium at the transition from exponential to stationary growth phase.

*Οερεξπρεσσιον οφ ΨβεΨ παρτιαλλψ ρεσσυεσ τηε ΔψβεΞ πηενοτψπε*

We used a constitutively expressed *E. coli* open reading frame (ORF) plasmid library representing 3974 ORFs, cloned in a multi-copy zeocin-resistant Gateway pENTR/Zeo plasmid (Rajagopala *et al.*, 2010), to search for genes that compensate for the deletion of *ybeX*. The selection was made in two independent experiments for three 12-hour rounds, resulting in enriched plasmid pools (**Fig. 9A**). We sequenced about 150 clones from the enriched plasmid pools. The *ybeY*-coding plasmid was predominant (>90%) among sequenced clones. Surprisingly, we did not recover a single *ybeX*-coding plasmid, suggesting the harmfulness of *ybeX* overexpression. Accordingly, the multi-copy *ybeX*-coding plasmid led to equally strong growth inhibition in WT and  $\Delta\psi\beta\epsilon\Xi$  cells (**Fig. S8a**). In contrast, the *ybeY*-coding plasmid had no visible detrimental effect on the growth of the  $\Delta\psi\beta\epsilon\Xi$  mutant.

We also measured growth in liquid LB medium. In this experiment, the multi-copy *ybeX* plasmid in the  $\Delta\psi\beta\epsilon\Xi$  background further increased the duration of the lag phase while also leading to a lower plateau of the growth curve (**Fig. S8b**). In contrast, the multi-copy *ybeY* plasmid in the  $\Delta\psi\beta\epsilon\Xi$  background partially rescues the lag phase phenotype (**Fig. S8b**). In the light of this partial rescue of the  $\Delta\psi\beta\epsilon\Xi$  phenotype by the multi-copy *ybeY* coding plasmid, we next tested whether overexpression of YbeY from an inducible pET-based multi-copy plasmid under the control of the taq promoter can further rescue the  $\Delta\psi\beta\epsilon\Xi$  lag phenotype. We found that overexpression of YbeY in  $\Delta\psi\beta\epsilon\Xi$  strain in the presence of 1 mM IPTG did not result in complete rescue of the  $\Delta\psi\beta\epsilon\Xi$  lag phase phenotype (**Fig. 9B**).

We further tested whether overexpression of YbeX and YbeY from a single-copy TransBac library plasmid influences the growth of  $\Delta\psi\beta\epsilon\Xi$  phenotype (**Fig. 9C**). Overexpression of YbeX and YbeY conferred no growth effect on WT cells. When induced in  $\Delta\psi\beta\epsilon\Xi$  cells, the single-copy *ybeY* plasmid compensated for the lack of chromosomal *ybeY*. In contrast, overexpression of YbeX in  $\Delta\psi\beta\epsilon\Xi$  cells led to a strong growth-rate reduction and a markedly lower final culture density.

Further, we conjugated the TransBac library plasmid overexpressing YbeX into three additional Keio deletion strains of genes whose products are associated with 30S ribosomal assembly. Deletion of *rimM* and *yjeQ* is known to impede growth at 37°C, while *ksqA* deletion does not affect bacterial growth at 37°C (Shajani *et al.*, 2011). We found that the growth of  $\Delta\kappa\sigma\gamma A$  was not significantly affected by YbeX overexpression, while  $\Delta\rho\mu M$  and  $\Delta\psi\theta\epsilon X$  strains exhibited growth inhibition (**Fig. 9D, E**). Therefore, sensitivity to *ybeX* overexpression is not a YbeY-specific phenomenon but seems to be associated with defective ribosomal assembly in general.

## DISCUSSION

This work shows that the putative  $Co^{2+}/Mg^{2+}$  efflux protein YbeX is functionally involved in ribosome metabolism in *E. coli*. For a possible mechanism that is consistent with experimental results, we propose

that growth without YbeX leads to the accumulation of 17S pre-rRNA and 16S rRNA partial degradation intermediates in the late-exponential growth phase (**Fig. 6B-F**), which necessitates a longer lag phase upon outgrowth in a fresh medium. During this prolonged lag phase (**Fig. 1C, Fig. 4B**), the  $\Delta\psi\beta\epsilon\Xi$  cells are metabolically active (**Fig. 1D**) and would be busy cleaning up the inactive and/or partially degraded ribosomal particles before new ribosome synthesis and subsequent cell division can commence (**Fig. 5B-E**). During the transition from exponential growth to stationary phase, lack of the YbeX leads to sensitivity to erythromycin, chloramphenicol, tetracycline, clindamycin and fusidic acid, which are known to induce cold-shock proteins or block the induction of heat-shock proteins (**Fig. 3A, Fig. 8**). Although the late-exponential phase  $\Delta\psi\beta\epsilon\Xi$  cells accumulate rRNA degradation products, to some extent, even in the 70S fraction (**Fig. 6B, D**), they have WT-like sucrose gradient profiles (**Fig. 6A**), indicating no accumulation of significant defective ribosome-like particles. In addition, the exponential growth rate of the  $\Delta\psi\beta\epsilon\Xi$  cells is indistinguishable from WT, as are the growth end-points (**Fig. 1C, Fig. 7C, Fig. 8B**).

The involvement of the YbeX in ribosomal metabolism is further supported by the partial rescue of its deletion phenotype by overexpression of YbeY (**Fig. 9B**), which is part of the *ybeZYX* operon and involved in ribosomal small subunit assembly and degradation, possibly through its enzymatic activity (Liao *et al.*, 2021). Although generally milder, *ybeX* deletion in *E. coli* leads to overlapping phenotypes with *ybeY* deletion. This raises the question of whether the products of these genes might work in the same pathway of ribosomal metabolism. Both YbeY and the YbeX exert an influence on cell growth through their effects on the ribosomal assembly and/or degradation of rRNA. One could posit a possible auxiliary role of YbeX in support of YbeY function. However, the function of the metalloprotein YbeY, with its zinc cofactor, remains enigmatic, primarily due to the lack of *in vivo* experimental data. Our results showing opposite effects on YbeX overexpression in  $\Delta\psi\beta\epsilon\Psi$  background and YbeY overexpression in  $\Delta\psi\beta\epsilon\Xi$  background (**Fig. 9B, C**) are logically inconsistent with causal schemes where YbeX and YbeY work in a single pathway, one after another, to influence cell growth.

The *ybeX/corC* gene was discovered in a *Salmonella enterica* serovar *Typhimurium* screen for resistance to cobalt. It was proposed that CorC contributes to the efflux of divalent cations, possibly by sensing cations or as a co-effector of CorA (Gibson *et al.*, 1991). As yet, there is no mechanistic function ascribed to YbeX, and while  $Mg^{2+}$  influx is generally well-studied, its efflux is poorly understood in bacteria (Armitano *et al.*, 2016). Essentially, YbeX is a cytoplasmic protein (Sueki *et al.*, 2020), for which we have no direct evidence that it might be involved in  $Mg^{2+}$ -efflux. The anticipated phenotype for a magnesium efflux mutant would be sensitivity to increased magnesium levels. In contrast, *ybeX* null mutant phenotypes were rescued in our experiments when cells were exposed to high magnesium, reaching as high as 100 mM  $MgCl_2$  (**Fig. 7A, Fig. S7a**). Thus, our findings are inconsistent with a magnesium protective role for YbeX in *E. coli*. Intriguingly, the rescue of growth of the  $\Delta\psi\beta\epsilon\Xi$  strain by  $MgCl_2$  occurs through a threshold effect, whereby something happens between 50  $\mu M$  and 75  $\mu M$   $MgCl_2$  that essentially abolishes the phenotype (**Fig. 7C, Fig. S6d, e**). Understanding the role of YbeX in  $Mg^{2+}$  metabolism requires more experimental work.

What could be the mechanistic role of YbeX in the *E. coli* cell? Unlike its neighboring gene products, YbeZ and YbeY, there is no evidence that YbeX binds to the ribosome or any ribosome-associated proteins. The transition from the exponential phase to the stationary phase, where *ybeX* mutant phenotypes are prominent, results in the degradation of the ribosome (Piir *et al.*, 2011). A recent study using rRNA-FISH in *E. coli* and *Salmonella* shows a heterogeneous 16S rRNA decrease occurs during this growth transition, stabilizing into low-uniform levels in the stationary phase (Ciolli Mattioli *et al.*, 2023). This observation could account for the colony heterogeneity in  $\Delta\psi\beta\epsilon\Xi$  strain; while a subpopulation of cells regrows faster because ribosomes are efficiently degraded, the remaining cells tend to form relatively smaller colonies because of ineffective clearance of the toxic rRNA fragments from the cell (**Fig. 2B, Fig. 5B-E**). It is plausible that YbeX is needed for efficient processing and removal of rRNA decay intermediates. According to this hypothesis, during the lag phase preceding exit from the stationary phase, exponential growth starts after the degradation of the decay intermediates is completed.

Overall, our results indicate a role for YbeX in ribosome assembly and/or rRNA degradation under

magnesium-limited conditions. The specific molecular mechanisms underlying the function of YbeX are yet to be elucidated.

## EXPERIMENTAL PROCEDURES

### Bacterial Strains, Plasmids and Growth Media

Genotypes of the bacterial strains, plasmid descriptions, and sequences of primers used in this study are listed in Tables S2-S3. Bacteria were grown in Difco™ LB Broth (BD #240230) consisting of 10 g/L tryptone, 5 g/L yeast extract, and 5 g/L sodium chloride. LB agar plates were prepared from Difco™ LB Agar (BD #240110). The growth media was supplemented with an appropriate amount of antibiotics (100 µg/mL ampicillin or carbenicillin, 25 µg/mL chloramphenicol, 50 µg/mL kanamycin, 12.5 µg/mL tetracycline, 25-50 µg/mL zeocin) when necessary for the selection of strains and maintenance of plasmids.

Keio collection strains, including  $\Delta\psi\beta\epsilon\Xi$ ,  $\Delta\psi\beta\epsilon\Psi$ ,  $\Delta\psi\beta\epsilon Z$ ,  $\Delta\rho\mu M$ ,  $\Delta\psi\theta\epsilon X$  and  $\Delta\kappa\sigma\gamma A$ , and *Escherichia coli* wild-type BW25113 were used in this study (Baba *et al.*, 2006). We also reconstructed the *ybeX* single deletion mutant using *E. coli* MG1655 and BW25113 via lambda red recombination (Datsenko and Wanner, 2000). The kanamycin resistance gene (kan) was removed from the bacterial chromosome using the pCP20 plasmid.

*E. coli*  $\Delta H5a$  strain was used for plasmid cloning and propagation. The TransBac library, an unpublished new *E. coli* overexpression library based on a single-copy vector, was obtained from Dr Hirotada Mori (Nara Institute of Science and Technology, Japan) as a stab stock (Otsuka *et al.*, 2015).

### Conjugation of the TransBac library plasmids

*Hfr*<sup>+</sup> strain (*E. coli* F+*dapA*<sup>-</sup> strain; BW38029 Hfr (CIP8*oriT::cat*) *dap*<sup>-</sup>) is the donor strain that carries each TransBac library plasmid and can transfer the target plasmid by conjugation (Otsuka *et al.*, 2015; Bobonis *et al.*, 2022). The donor strain was grown on LB agar plates supplemented with 12.5 µg/mL tetracycline (Tc) and 25-50 µg/mL diaminopimelic acid (Acros Organics, #235540050). *Hfr*<sup>+</sup> donor strains require DAP to grow because of the deletion of the *dapA*. Well-grown donor and acceptor cells were mixed (1:1) in a 1.5 mL polypropylene tube and incubated at 37°C for 1 hour without shaking. The recovery step was carried out in SOC medium for 1 hour at 37°C 850 rpm shaking thermostat (Eppendorf Thermomixer compact), and the cells were spread onto LB agar plates containing only Tc without DAP. The plates were incubated at 37°C overnight. The ORFs were sequenced using ISM43 (TTA AAG AGG AGA AAC CTA GG) and ISM44 (CTT AGC GGC CGC ATA).

### Construction of the TransBac empty (pTB-empty) plasmid

The single-copy TransBac library plasmid coding *ybeX* was purified using an in-house alkaline lysis method followed by purification via FavorPrep plasmid DNA extraction mini kit (Favorgen, #FAPDE300). The cloning site was sequenced by Sanger sequencing (University of Tartu). The *ybeX* coding region was removed via restriction enzyme cleavage of FastDigest *Xma*II and *Sfi*I (Thermo Scientific). The sticky ends were filled using Klenow fragment (Thermo Scientific), and the linear plasmid was ligated using T4 DNA ligase (Thermo Scientific) following manufacturer protocols. The ligation reaction was transformed into Inoue *E. coli*  $\Delta H5a$  chemical competent cells (Green and Sambrook, 2020), and the TransBac empty backbone plasmid was purified as mentioned above. The size of the plasmid DNA was determined via agarose gel electrophoresis, and the cloning site was sequenced using SO10 primer (see Table S3). The plasmid was electroporated into wild-type and  $\Delta\psi\beta\epsilon\Xi$  strains.

### Preparation of the Peptide Based Medium (PBM)

Growth in a peptide-based medium (PBM) is magnesium-limited (Christensen *et al.*, 2017). The previously described PBM recipe requires extra glucose (4 g/L) as a carbon source. Instead, we prepared the PBM by dissolving 10g/L Peptone, 1.5% casein hydrolysate (casamino acids) and 40 mM MOPS buffer pH 7.4. The 50x MOPS buffer stock solution contained 2 M MOPS (3-(N-morpholino) propane sulfonic acid) and 0.2 M

tricine pH 7.4 set with concentrated KOH. We achieved very high cell densities,  $OD_{600} = 12-13$ , when 2x PBM was supplemented with 1-10 mM  $MgCl_2$  or  $MgSO_4$ .

### Bacterial Spot Assay

Bacterial cell cultures were diluted to final  $OD_{600} = 0.125$ , the first dilution ( $10^{-1}$ ), and then 10x serial dilutions were applied. 5 $\mu$ L of each dilution were spotted on LB agar plates with or without antibiotics (No AB). The sub-MIC (sub-inhibitory) concentrations of the antibiotics were as follows: 2.5-4  $\mu$ g/mL chloramphenicol; 0.5-1  $\mu$ g/mL tetracycline; 25-40  $\mu$ g/mL erythromycin; 50  $\mu$ g/mL clindamycin; 100  $\mu$ g/mL fusidic acid; 10  $\mu$ g/mL mupirocin; 0.5  $\mu$ g/mL tobramycin or amikacin; 2.5  $\mu$ g/mL rifampicin or streptomycin. The plates were imaged using an Epson Expression 1680-pro scanner. In Fig. 9D, R2A agar (VWR, #84671.0500) plates were used to test the slow regrowth of bacterial cells from the MOPS minimal medium. R2A Agar is a low-nutrient medium, and in combination with a longer incubation time, it stimulates the growth of stressed bacteria.

### Colony Size Characterization and Quantification

Keio wild-type and  $\Delta\psi\beta\epsilon\Xi$  strains were grown overnight in LB or defined MOPS minimal medium (Neidhardt *et al.*, 1974). Well-grown bacterial cell cultures were serially diluted and plated on LB agar plates using glass beads (Hecht Assistent, #41401004). We aimed to have approximately 100-125 colonies per plate. The plates were incubated overnight at 37°C or 42°C and scanned using EPSON Expression 1680pro scanner. The images were subjected to AutoCellSeg software (Khan *et al.*, 2018). The colonies were first picked automatically using program default settings, and then, as a second step, manual picking was applied (picking small colonies, deselecting adherent colonies, etc.). The data were analyzed in the R packages tidyverse and visualized with ggplot2 (Wickham *et al.*, 2019; R Core Team, 2022).

### Growth monitoring in the 96-well plate reader

Cells were diluted in the appropriate growth media to  $OD_{600} = 0.55$ , and 10  $\mu$ L of the diluted cells were transferred into 100  $\mu$ L of growth medium in a 96-well plate (Anicrin, Flat bottom, #18EMP.I.). The 96-well plate edges were filled with distilled water or 1xPBS. The remaining 60 wells were used to monitor the growth. At least one column was always set as a sterility control. Alamar Blue reagent (BioRad, #BUF012B) was used per the manufacturer's protocol (excitation 545 nm, emission 590 nm). BioTek Synergy MX or H1 microplate readers were used.

### Purification of the pooled E. coli K-12 ORFeome plasmid library

A previously described *E. coli* ORFeome plasmid library (Rajagopala *et al.*, 2010) was received as a stab stock in a 96-well plate format (National BioResource Project, Japan). The clones were grown in LB medium supplemented with 50  $\mu$ g/mL Zeocin for 24 hours at 37°C (Velp Scientifica FTC 90I). The cell cultures were pooled, and the plasmids were purified using a NucleoBond Xtra Midi kit (Macherey-Nagel).

### Library selection experiment

The purified plasmid library was electroporated into  $\Delta ybeX::kan$ . The cells were recovered in LB medium for 1 hour at 37°C 850 rpm shaking thermostat (Eppendorf Thermomixer compact). The recovery culture was diluted in LB medium supplemented with 50  $\mu$ g/mL Zeocin and grown for 12 hours at 37°C 200 rpm shaking (Infors HT Minitron shaker). After 12 hours, the cell cultures were diluted 100x in fresh LB containing 50  $\mu$ g/mL Zeocin and grown for an additional 12 hours at 37°C. The previous step was repeated, and the plasmids were purified at every stage (12h, 24h, and 36h). The purified plasmid pools were cleaved via FastDigest SfiI (Thermo Scientific) restriction enzyme at 50°C. Excision of the ORF inserts of the plasmid pools revealed in agarose electrophoresis several bands, of which the most prominent was slightly over 500 kb (**Fig. S8c**). The enriched plasmid pools were transformed in DH5 $\alpha$  Inoue chemical competent cells (Green and Sambrook, 2020) and plated on LB agar plates containing 25  $\mu$ g/mL Zeocin (Invivogen). Colony PCR was performed using ISM1 (GGC TTG GCC CTG AGG GCC) and ISM2 (GTG GCG GCC GCA TAG GCC) primers following manufacturer protocol for Hot FirePol<sup>®</sup> blend master mix ready to load (Solis

BioDyne, #04-25-00115). The PCR cycling parameters were 95°C 12 min, (95°C 20 sec, 56°C 60 sec, 72°C 20 sec/kb) × 28 cycles, 72°C 10 min, and 15°C infinite hold. PCR products were sequenced via Sanger sequencing (University of Tartu).

#### Construction of pET-based YbeY overexpression plasmid

The pET-ybeY overexpression plasmid was constructed using the CPEC (Circular Polymerase Extension Cloning) method (Quan and Tian, 2011). The primers were designed to amplify the pET-Orange plasmid backbone and the coding region of the *ybeY* gene from the *E. coli* genome (sequences are detailed in Table S3). Phusion HF DNA Polymerase (Thermo Scientific, #F530L) was used following the manufacturer protocol.

#### Sucrose gradient fractionation

*E. coli* strains from the Keio collection were streaked onto LB agar plates and grown overnight at 37degC. A single colony of each strain was inoculated into LB and aerated at 37degC overnight. The following morning, the culture densities were determined via spectrophotometer (Biochrom Ultrospec 7000); the cells were diluted to a final OD<sub>600</sub> of 0.05-0.06 in LB medium (150-250mL) and grown until OD<sub>600</sub> = 0.3-0.35. The cultures were then split into two flasks, in which the chloramphenicol treatment was carried out, while the other was grown as a control for 2 hours.

The cells were transferred into centrifugation bottles, cooled on ice and pelleted at 4000xg, at +4degC for 10 minutes. The supernatant was removed, and the cell pellet was snap-frozen in liquid nitrogen and stored at -80degC. For cell lysis, the frozen cell pellets were thawed on ice and then taken up in 1 mL of lysis buffer consisting of 25 mM Tris-HCl pH 7.9, 60 mM KCl, 60 mM NH<sub>4</sub>Cl, 6 mM MgCl<sub>2</sub>, 5% glycerol supplemented with 1mM PMSF, protease inhibitor (Roche, #04693159001) and 5mM βME added freshly to the buffer. The cells were lysed using FastPrep homogenizer (MP Biomedicals) by three 40-second pulses at 4.0 m/s, chilling on ice for 5 min between the cycles. The beads were purchased from BioSpec Products, and 0.4 gram of 0.5mm Zirconia/Silica beads (BioSpec, #11079105z) and 0.9 gram of 0.1mm Zirconia/Silica beads (BioSpec, #11079101z) was used.

The lysate was clarified by centrifugation 16,100xg for 40 minutes at +4°C. Clarified lysates were treated with 50 units/mL DNase I (MN, #740963) on ice and centrifuged for 10 minutes as above. The AU<sub>260</sub> was monitored, and 50U was loaded. The lysates were loaded onto 10-30% sucrose gradients in a buffer containing 25 mM Tris-HCl pH 7.9, 100 mM KCl, 10 mM MgCl<sub>2</sub>, supplemented with 5mM βME. The gradients were centrifuged at 20,400 rpm for 17 h at +4°C in an SW-28 Beckman Coulter rotor ( $\omega^2t=2.8e+11$ ). The samples from the gradient were pumped from the bottom through a spectrophotometer (Econo UV Monitor, BIO-RAD), which can detect absorbance at 254 nm as a readout. The data was recorded by Data Acquisition software (DataQ Instruments) and imported into R for plotting (R Core Team, 2022).

#### Purification of rRNA from Ribonucleoprotein (RNP) Complexes

Ribosomes and ribosomal subunits were manually collected from sucrose gradients as peak fractions. The sucrose fractions were collected into 15 mL falcon tubes and diluted at least two-fold with the gradient buffer (25 mM Tris-HCl pH 7.9, 100 mM KCl, 10 mM MgCl<sub>2</sub>). Next, 2.5 vol. of 96% ethanol was added to the samples and incubated at -20°C overnight. The fractions were pelleted via centrifugation for 45 minutes at 4000 rpm +4°C (4K15 Sigma, rotor 11150). The pellet was washed with 70% EtOH, and centrifugation was re-applied for 10 minutes. The ribonucleoprotein complexes were suspended in 0.1 mL of MilliQ water, and samples were stored at -20°C.

The rRNA was purified with phenol-chloroform extraction. The samples were kept on ice, and 1% SDS-containing phenol was added to the samples. Samples were vortexed vigorously for 10 s, kept on ice for 5 min, and centrifuged at 16,100xg 10 min at +4°C. The water phase was transferred to a new microfuge tube into which chloroform:phenol mixture (1:1) was added and vortexed for 10 seconds, centrifuged as above. This step was repeated, using only chloroform to avoid phenol carryover. The water phase was transferred to a new microfuge tube, and the RNA was precipitated with 0.1 vol. 3M sodium acetate (pH 5.2-5.5) and

2.5 vol. ethanol at  $-20^{\circ}\text{C}$  for 1 hour. The pellet was washed with 70% EtOH and dried at room temperature for 5 minutes. The purified RNA was dissolved in ultra-pure distilled water (MilliQ).

#### Total RNA Purification using hot phenol extraction

The strains were grown in LB at  $37^{\circ}\text{C}$ . 10-12 mL of cell culture were transferred to a 15 mL Falcon tube, pelleted via centrifugation at 8000xg for 3-4 minutes, snap-frozen in liquid nitrogen, and stored at  $-80^{\circ}\text{C}$  until RNA purification. Total RNA was purified with hot phenol-chloroform extraction, as described previously (Kasari *et al.*, 2013).

#### Denaturing Agarose Gel Electrophoresis

The isolated RNA samples were separated by denaturing 1.5% agarose gel containing 1xMOPS buffer and 2% formaldehyde. 5  $\mu\text{g}$  of RNA (no more than 6.6  $\mu\text{L}$  in final volume) was mixed with 5.4  $\mu\text{L}$  of formaldehyde, 3  $\mu\text{L}$  of 10x MOPS buffer and 15  $\mu\text{L}$  of formamide. The samples and RNA markers from Thermo Scientific (RiboRuler High Range, #SM1821 and Low Range RNA ladder, # SM1831) were denatured at  $55^{\circ}\text{C}$  for 15 minutes. The RNA mixes were then cooled on ice. Sample loading dye (5 $\mu\text{L}$ , 1:6) (0.25% bromophenol blue, 40% sucrose) was added to the samples, and the samples were loaded. The electrophoresis buffer was the same as the buffer used to prepare the gel, 1 x MOPS. During the first hour, 60V was applied, and the voltage was increased to 85V.

After 5 hours, when the run ended, the ladder region was cut off and stained for 30 min in the running buffer containing 5000x diluted Diamond Nucleic acid dye (Promega). The transfer of the RNA from the agarose gel to the nylon membrane (Amersham Hyband-N+, GE Healthcare, #RPN303B) was done via capillary transfer of RNA from the denaturing agarose gel to the nylon membrane (Sambrook, 2001). RNA crosslinking to the nylon membrane was done via UV (Stratagene crosslinker).

#### The hybridization of the Northern Blot Membrane

25 mL hybridization buffer (0.5 M sodium phosphate buffer pH 7.2 containing 7% SDS) and the rotating bottle were heated in a hybridization oven (Hybrigen Techne FHB4DP, #3945507) at  $62^{\circ}\text{C}$  in darkness. The nylon membrane was placed in the bottle and rotated for two hours. The fluorescent-labelled DNA oligonucleotide was added at the 2 nM final concentration, and hybridization occurred overnight. The next day, the wash buffer (20 mM sodium phosphate buffer pH 7.2 containing 1% SDS) was warmed in a water bath to  $43^{\circ}\text{C}$ . The membrane was washed with 250 mL of pre-warmed wash buffer at  $43^{\circ}\text{C}$  thrice for 5 minutes on an orbital shaker in a metal box, preventing light exposure. Finally, the membrane was placed into a plastic envelope. The scanning of the membrane was done in the Amersham Typhoon laser scanner.

#### Statistical analysis

A two-sided Student's t-test with unequal variances (Welch's t-test) was done in GraphPad Prism version 5.01 (GraphPad Software, San Diego, CA, USA). Other statistical analyses were done in R vers. 4.2.1 (R Core Team, 2022). The Alamar Blue and corresponding  $\text{OD}_{600}$  measurements shown in Fig. 1 and Fig. S2 were modelled with splines using the *bamlss* package version 1.1-8 (Umlauf *et al.*, 2021). The modelling was done separately for each strain and condition (Alamar Blue fluorescence signal and  $\text{OD}_{600}$  signal). The model description is *bamlss*(value ~ s(Time\_min), family="gaussian"). The growth curves in Fig. 4, 7, and 9 were done using the *growthcurver* package and ggplot2 (Wickham, 2016; Sprouffske and Wagner, 2016). All figures were plotted using R/ggplot2 in RStudio, except in Fig. 8B using GraphPad.

#### ACKNOWLEDGEMENTS

We thank Dr Hirotada Mori (Nara Institute of Science and Technology, Japan) for sending us the unpublished TransBac plasmid library. This work was supported by funds from the European Regional Development Fund through the Centre of Excellence for Molecular Cell Technology and the Estonian Research Council (grant PRG335).

#### AUTHOR CONTRIBUTIONS

U.M., T.T. conceived the study. Ī.S., Ū.M., and T.T. designed the research. Ī.S., E.A. and A.Ž. conducted the experiments. Ī.S., Ū.M., and M.P. analyzed the data. Ī.S. prepared all figures and tables. Ī.S. and Ū.M. wrote the original draft. T.T., S.R., and N.K. reviewed and edited the manuscript. All authors read and approved the manuscript.

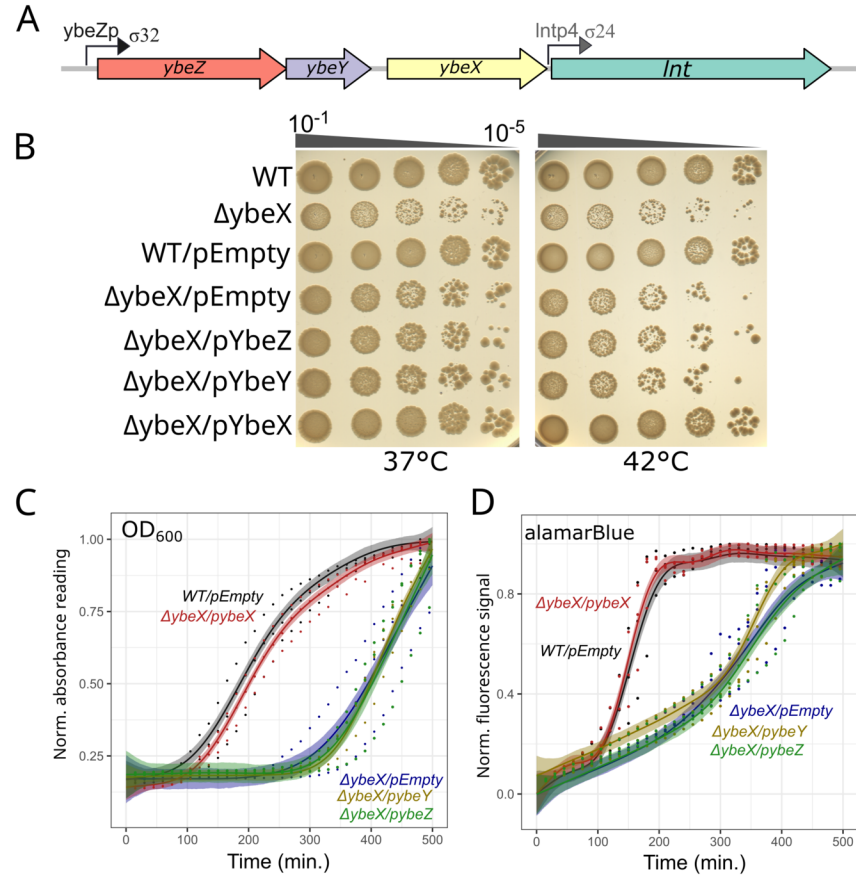
## REFERENCES

- Anantharaman, V., and Aravind, L. (2003) Application of comparative genomics in the identification and analysis of novel families of membrane-associated receptors in bacteria. *BMC Genomics* **4** : 34.
- Andrews, E.S.V., and Patrick, W.M. (2022) The hypothesized role of YbeZ in 16S rRNA maturation. *Arch Microbiol* **204** : 114.
- Armitano, J., Redder, P., Guimarães, V.A., and Linder, P. (2016) An Essential Factor for High Mg<sup>2+</sup> Tolerance of *Staphylococcus aureus*. *Front Microbiol* **7** : 1888.
- Baba, T., Ara, T., Hasegawa, M., Takai, Y., Okumura, Y., Baba, M., *et al.* (2006) Construction of *Escherichia coli* K-12 in-frame, single-gene knockout mutants: the Keio collection. *Mol Syst Biol* **2** : 2006.0008.
- Babu, V.M.P., Sankari, S., Budnick, J.A., Caswell, C.C., and Walker, G.C. (2020) Sinorhizobium meliloti YbeY is a zinc-dependent single-strand specific endoribonuclease that plays an important role in 16S ribosomal RNA processing. *Nucleic Acids Res* **48** : 332–348.
- Bobonis, J., Mitosch, K., Mateus, A., Karcher, N., Kritikos, G., Selkrig, J., *et al.* (2022) Bacterial retrons encode phage-defending tripartite toxin–antitoxin systems. *Nature* **609** : 144–150.
- Butland, G., Peregrín-Alvarez, J.M., Li, J., Yang, W., Yang, X., Canadien, V., *et al.* (2005) Interaction network containing conserved and essential protein complexes in *Escherichia coli*. *Nature* **433** : 531–537.
- Caglar, M.U., Houser, J.R., Barnhart, C.S., Boutz, D.R., Carroll, S.M., Dasgupta, A., *et al.* (2017) The *E. coli* molecular phenotype under different growth conditions. *Sci Rep* **7** : 45303.
- Christensen, D.G., Orr, J.S., Rao, C.V., and Wolfe, A.J. (2017) Increasing Growth Yield and Decreasing Acetylation in *Escherichia coli* by Optimizing the Carbon-to-Magnesium Ratio in Peptide-Based Media. *Applied and Environmental Microbiology* <https://journals.asm.org/doi/abs/10.1128/AEM.03034-16>. Accessed January 25, 2022.
- Ciulli Mattioli, C., Eisner, K., Rosenbaum, A., Wang, M., Rivalta, A., Amir, A., *et al.* (2023) Physiological stress drives the emergence of a *Salmonella* subpopulation through ribosomal RNA regulation. *Current Biology* <https://www.sciencedirect.com/science/article/pii/S0960982223013131>. Accessed October 25, 2023.
- Cruz-Loya, M., Kang, T.M., Lozano, N.A., Watanabe, R., Tekin, E., Damoiseaux, R., *et al.* (2019) Stressor interaction networks suggest antibiotic resistance co-opted from stress responses to temperature. *ISME J* **13** : 12–23.
- Datsenko, K.A., and Wanner, B.L. (2000) One-step inactivation of chromosomal genes in *Escherichia coli* K-12 using PCR products. *PNAS* **97** : 6640–6645.
- Davies, B.W., Köhrer, C., Jacob, A.I., Simmons, L.A., Zhu, J., Aleman, L.M., *et al.* (2010) Role of *Escherichia coli* YbeY, a highly conserved protein, in rRNA processing. *Mol Microbiol* **78** : 506–518.
- Davis, J.H., and Williamson, J.R. (2017) Structure and dynamics of bacterial ribosome biogenesis. *Philosophical Transactions of the Royal Society B: Biological Sciences* **372** : 20160181.
- D’Souza, A.R., Van Haute, L., Powell, C.A., Mutti, C.D., Páleníková, P., Rebelo-Guiomar, P., *et al.* (2021) YbeY is required for ribosome small subunit assembly and tRNA processing in human mitochondria. *Nucleic Acids Research* <https://doi.org/10.1093/nar/gkab404>. Accessed May 28, 2021.

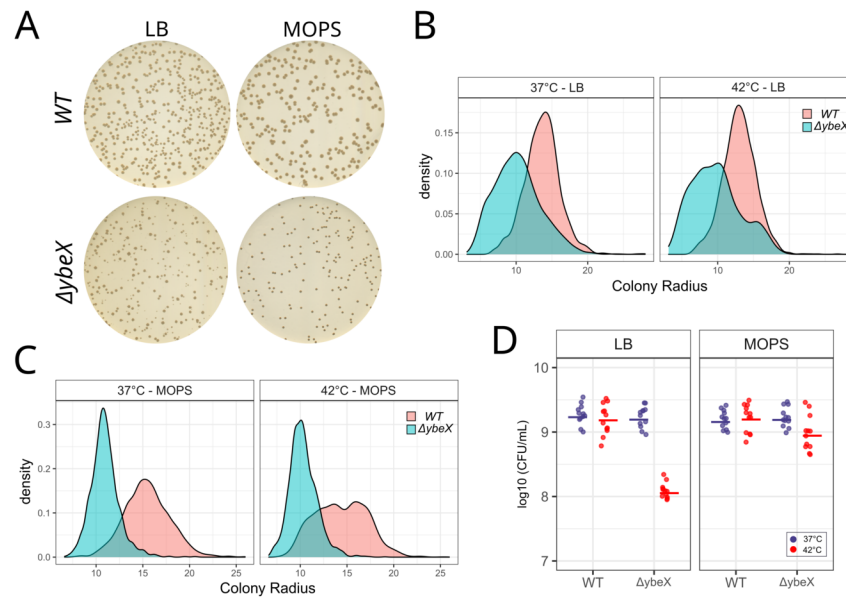
- Gibson, M.M., Bagga, D.A., Miller, C.G., and Maguire, M.E. (1991) Magnesium transport in *Salmonella typhimurium*: the influence of new mutations conferring Co<sup>2+</sup> resistance on the CorA Mg<sup>2+</sup> transport system. *Mol Microbiol* **5** : 2753–2762.
- Green, M.R., and Sambrook, J. (2020) The Inoue Method for Preparation and Transformation of Competent *Escherichia coli*: “Ultracompetent” Cells. *Cold Spring Harb Protoc* **2020** : pdb.prot101196.
- Jacob, A.I., Köhrer, C., Davies, B.W., RajBhandary, U.L., and Walker, G.C. (2013) Conserved bacterial RNase YbeY plays key roles in 70S ribosome quality control and 16S rRNA maturation. *Mol Cell* **49** : 427–438.
- Kasari, V., Mets, T., Tenson, T., and Kaldalu, N. (2013) Transcriptional cross-activation between toxin-antitoxin systems of *Escherichia coli*. *BMC Microbiology* **13** : 45.
- Kazakov, A.E., Vassieva, O., Gelfand, M.S., Osterman, A., and Overbeek, R. (2003) Bioinformatics classification and functional analysis of PhoH homologs. *In Silico Biol* **3** : 3–15.
- Keseler, I.M., Mackie, A., Peralta-Gil, M., Santos-Zavaleta, A., Gama-Castro, S., Bonavides-Martínez, C., *et al.* (2013) EcoCyc: fusing model organism databases with systems biology. *Nucleic Acids Res* **41** : D605–612.
- Khan, A. ul M., Torelli, A., Wolf, I., and Gretz, N. (2018) AutoCellSeg: robust automatic colony forming unit (CFU)/cell analysis using adaptive image segmentation and easy-to-use post-editing techniques. *Sci Rep* **8** : 7302.
- Kim, S.K., Makino, K., Amemura, M., Shinagawa, H., and Nakata, A. (1993) Molecular analysis of the *phoH* gene, belonging to the phosphate regulon in *Escherichia coli*. *Journal of Bacteriology* **175** : 1316–1324.
- Lee, D.D., Galera-Laporta, L., Bialecka-Fornal, M., Moon, E.C., Shen, Z., Briggs, S.P., *et al.* (2019) Magnesium Flux Modulates Ribosomes to Increase Bacterial Survival. *Cell* **177** : 352–360.e13.
- Li, R., Jin, M., Du, J., Li, M., Chen, S., and Yang, S. (2020) The Magnesium Concentration in Yeast Extracts Is a Major Determinant Affecting Ethanol Fermentation Performance of *Zymomonas mobilis*. *Front Bioeng Biotechnol* **8** : 957.
- Liao, Z., Schelcher, C., and Smirnov, A. (2021) YbeY, éminence grise of ribosome biogenesis. *Biochemical Society Transactions* **49** : 727–745.
- Liu, J., Zhou, W., Liu, G., Yang, C., Sun, Y., Wu, W., *et al.* (2015) The Conserved Endoribonuclease YbeY Is Required for Chloroplast Ribosomal RNA Processing in *Arabidopsis*1. *Plant Physiol* **168** : 205–221.
- McCarthy, B.J., Britten, R.J., and Roberts, R.B. (1962) The Synthesis of Ribosomes in *E. coli*: III. Synthesis of Ribosomal RNA. *Biophysical Journal* **2** : 57–82.
- Neidhardt, F.C., Bloch, P.L., and Smith, D.F. (1974) Culture Medium for Enterobacteria. *J Bacteriol* **119** : 736–747.
- Nonaka, G., Blankschien, M., Herman, C., Gross, C.A., and Rhodius, V.A. (2006) Regulon and promoter analysis of the *E. coli* heat-shock factor,  $\sigma_{32}$ , reveals a multifaceted cellular response to heat stress. *Genes Dev* **20** : 1776–1789.
- Orelle, C., Carlson, E.D., Szal, T., Florin, T., Jewett, M.C., and Mankin, A.S. (2015) Protein synthesis by ribosomes with tethered subunits. *Nature* **524** : 119–124.
- Otsuka, Y., Muto, A., Takeuchi, R., Okada, C., Ishikawa, M., Nakamura, K., *et al.* (2015) GenoBase: comprehensive resource database of *Escherichia coli* K-12. *Nucleic Acids Research* **43** : D606–D617.
- Piir, K., Paier, A., Liiv, A., Tenson, T., and Maiväli, Ü. (2011) Ribosome degradation in growing bacteria. *EMBO Rep* **12** : 458–462.

- Pontes, M.H., Yeom, J., and Groisman, E.A. (2016) Reducing Ribosome Biosynthesis Promotes Translation during Low Mg<sup>2+</sup> Stress. *Molecular Cell* **64** : 480–492.
- Quan, J., and Tian, J. (2011) Circular polymerase extension cloning for high-throughput cloning of complex and combinatorial DNA libraries. *Nat Protoc* **6** : 242–251.
- R Core Team (2022) *R: A Language and Environment for Statistical Computing*. R Foundation for Statistical Computing, Vienna, Austria. <https://www.R-project.org/>.
- Rajagopala, S.V., Yamamoto, N., Zweifel, A.E., Nakamichi, T., Huang, H.-K., Mendez-Rios, J.D., *et al.* (2010) The Escherichia coli K-12 ORFeome: a resource for comparative molecular microbiology. *BMC Genomics* **11** : 470.
- Rampersad, S.N. (2012) Multiple Applications of Alamar Blue as an Indicator of Metabolic Function and Cellular Health in Cell Viability Bioassays. *Sensors (Basel)* **12** : 12347–12360.
- Sambrook, J. (2001) *Molecular cloning : a laboratory manual*. Third edition. Cold Spring Harbor, N.Y. : Cold Spring Harbor Laboratory Press, [2001] (c)2001, . <https://search.library.wisc.edu/catalog/999897924602121>.
- Shajani, Z., Sykes, M.T., and Williamson, J.R. (2011) Assembly of Bacterial Ribosomes. *Annu Rev Biochem* **80** : 501–526.
- Siibak, T., Peil, L., Xiong, L., Mankin, A., Remme, J., and Tenson, T. (2009) Erythromycin- and Chloramphenicol-Induced Ribosomal Assembly Defects Are Secondary Effects of Protein Synthesis Inhibition. *Antimicrobial Agents and Chemotherapy* <https://journals.asm.org/doi/abs/10.1128/AAC.00870-08>. Accessed December 17, 2021.
- Smith, B.A., Gupta, N., Denny, K., and Culver, G.M. (2018) Characterization of 16S rRNA Processing with Pre-30S Subunit Assembly Intermediates from E. coli. *Journal of Molecular Biology* **430** : 1745–1759.
- Smith, L.K., Gomez, M.J., Shatalin, K.Y., Lee, H., and Neyfakh, A.A. (2007) Monitoring of gene knockouts: genome-wide profiling of conditionally essential genes. *Genome Biol* **8** : R87.
- Sprouffske, K., and Wagner, A. (2016) Growthcurver: an R package for obtaining interpretable metrics from microbial growth curves. *BMC Bioinformatics* **17** : 172.
- Sueki, A., Stein, F., Savitski, M.M., Selkrig, J., and Typas, A. (2020) Systematic Localization of Escherichia coli Membrane Proteins. *mSystems* **5** : e00808-19.
- Umlauf, N., Klein, N., Simon, T., and Zeileis, A. (2021) bamlss: A Lego Toolbox for Flexible Bayesian Regression (and Beyond). *J Stat Soft* **100** : 1–53.
- VanBogelen, R.A., and Neidhardt, F.C. (1990) Ribosomes as sensors of heat and cold shock in Escherichia coli. *Proceedings of the National Academy of Sciences* **87** : 5589–5593.
- Vercruyse, M., Kohrer, C., Shen, Y., Proulx, S., Ghosal, A., Davies, B.W., *et al.* (2016) Identification of YbeY-Protein Interactions Involved in 16S rRNA Maturation and Stress Regulation in Escherichia coli. *mBio* **7** .
- Wickham, H. (2016) *ggplot2: Elegant Graphics for Data Analysis*. 2nd ed. 2016., Springer International Publishing : Imprint: Springer, Cham.
- Wickham, H., Averick, M., Bryan, J., Chang, W., McGowan, L.D., Francois, R., *et al.* (2019) Welcome to the Tidyverse. *Journal of Open Source Software* **4** : 1686.
- Wilson, D.N. (2014) Ribosome-targeting antibiotics and mechanisms of bacterial resistance. *Nat Rev Microbiol* **12** : 35–48.

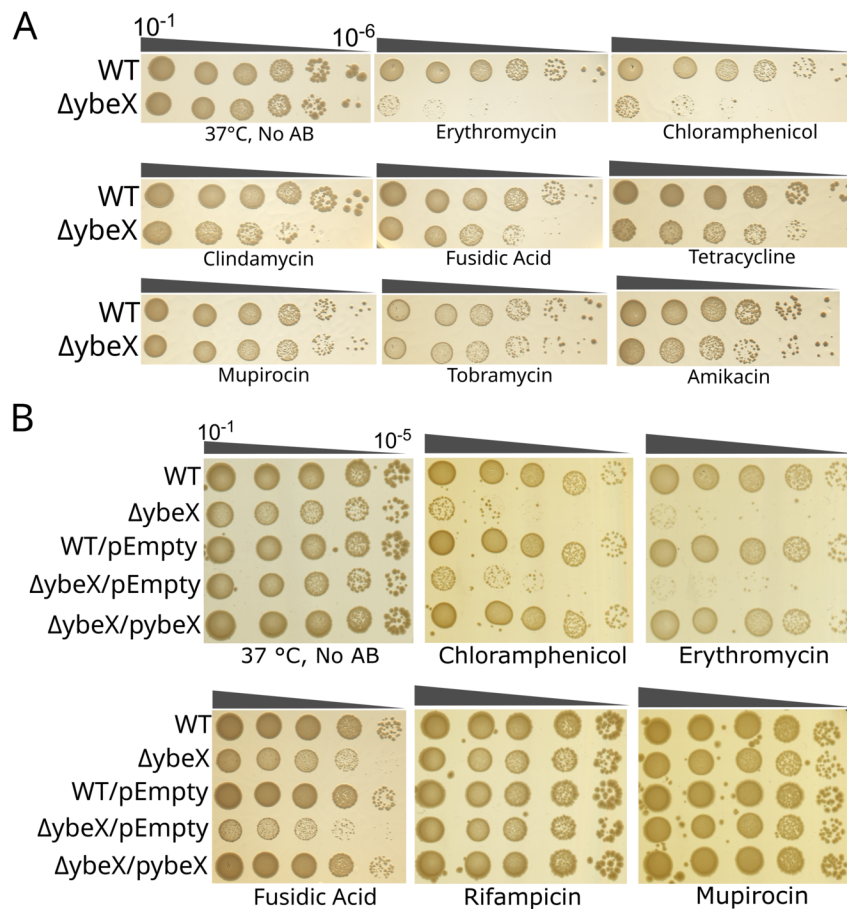
Xia, Y., Weng, Y., Xu, C., Wang, D., Pan, X., Tian, Z., *et al.*(2020) Endoribonuclease YbeY Is Essential for RNA Processing and Virulence in *Pseudomonas aeruginosa*. *mBio* **11** .



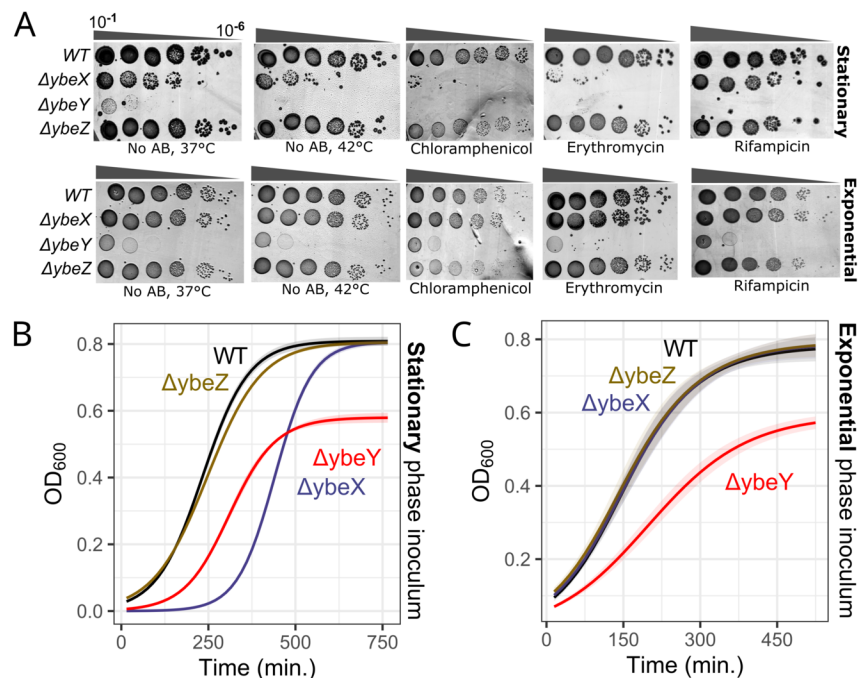
**Φιγ. 1.** Γρωιτη πηενοτψπεσ οφ  $\Delta\psi\beta\epsilon\Xi$  στραιν ανδ ζομπενσαιον ωιτη σινγλε-ζοπψ πλασμιδ. (A) The *E. coli ybeZYX-lnt* operon chromosomal organization with sigma factors ( $\sigma^{32}$  and  $\sigma^{24}$ ) and promoters (*ybeZp* and the predicted *lntp4*). (B) Dot spot assay of wild-type (WT) and  $\Delta\psi\beta\epsilon\Xi$  strains, along with the strains harbouring the TransBac library plasmid backbone (WT/pEmpty or  $\Delta\psi\beta\epsilon\Xi$ /pEmpty), and the  $\Delta\psi\beta\epsilon\Xi$  strain with the YbeZ, YbeY, or YbeX-expressing single-copy TransBac library plasmid. LB agar plates were incubated at 37°C or 42°C. (C-D) The stationary phase outgrowth of the wild type and the  $\Delta\psi\beta\epsilon\Xi$  strains in liquid LB medium. Panel C shows the OD<sub>600</sub> signal, and panel D shows the Alamar Blue fluorescence reading. Both signals are normalized to one. Individual measurements from independent experiments, each presented as the mean of three technical replicates, are shown as dots. Curves are modelled with splines, and 95% credible intervals are shown as shaded areas (see Materials and Methods for details). *pybeX*, *pybeZ* and *pybeY* denote the YbeX, YbeZ and YbeY expressing plasmid.



**Φιγ. 2.** Ηαρααααααααααα ααα αααααααααα αα  $\Delta\psi\beta\epsilon\Xi$  ααα  $\text{Κειο ωιλδ-αψαε}$  ( $\Omega\text{T}$ ) ααααα ααααα ααα 37°α αααα 42°α. (**A**) Representative LB agar plates with colonies of WT and  $\Delta\psi\beta\epsilon\Xi$  strains. As indicated on the panel's top, the cells were plated from LB or MOPS minimal media and the agar plates were incubated at 37°C overnight. (**B-C**) Density plots of the distribution of quantified colony radii of  $\Delta\psi\beta\epsilon\Xi$  and isogenic WT strains at 37°C and 42°C. The colonies were quantified from three independent experiments as of the plates in panel A. (**D**) Colony counts for WT and  $\Delta\psi\beta\epsilon\Xi$  strains grown in LB or MOPS minimal media as in panel A. Values of four biological replicates with three technical replicates each are shown.



**Φιγ. 3. ΔψβεΞ ζελλς εξηιβι σερρ σενσιτιψ το συβ-ΜΙ<sup>α</sup> ζονζεντρατιονς οφ ζολδ-σηοσκ-ινδυσινγ, ριβοσομε-βινδινγ αντιβιοτιςς.** (A ) The wild-type (WT) and the ΔψβεΞ cells were grown overnight in LB liquid medium, serially diluted, and spotted on LB agar plates supplemented with sub-MIC concentrations of indicated antibiotics (No AB). The plates were incubated at 37°C overnight. (B ) Representative images are given from a dot spot assay with strains described in Fig. 1. pYbeX denotes the YbeX-expressing TransBac library plasmid.



**Φιγ. 4.** Τη  $\Delta\psi\beta\epsilon\Xi$ -δεπενδεντ αντιβιοτис σενσιτιτψ ανδ ουτγρωτη δελαψ δεπενδ ον τη γρωτη πηασε οφ τη ινοσυλυμ. (A) Drops of the stationary phase and exponential phase cultures of the Keio wild-type (WT),  $\Delta ybeX$ ,  $\Delta ybeZ$ , and  $\Delta ybeY$  strains were spotted on LB-agar plates. The cells were cultured in LB medium, and the LB agar plates were incubated at 37°C, except for the 42°C plates. (B-C) Stationary and exponential phase cells of wild-type,  $\Delta ybeY$ ,  $\Delta ybeZ$ , and  $\Delta ybeX$  strains were inoculated into liquid LB medium, and the growth was monitored by measuring OD<sub>600</sub> at 37°C using a 96-well plate reader. The growth curves, summarizing three independent experiments, are shown as fitted logistic curves. Shaded areas represent the 95% CI-s.

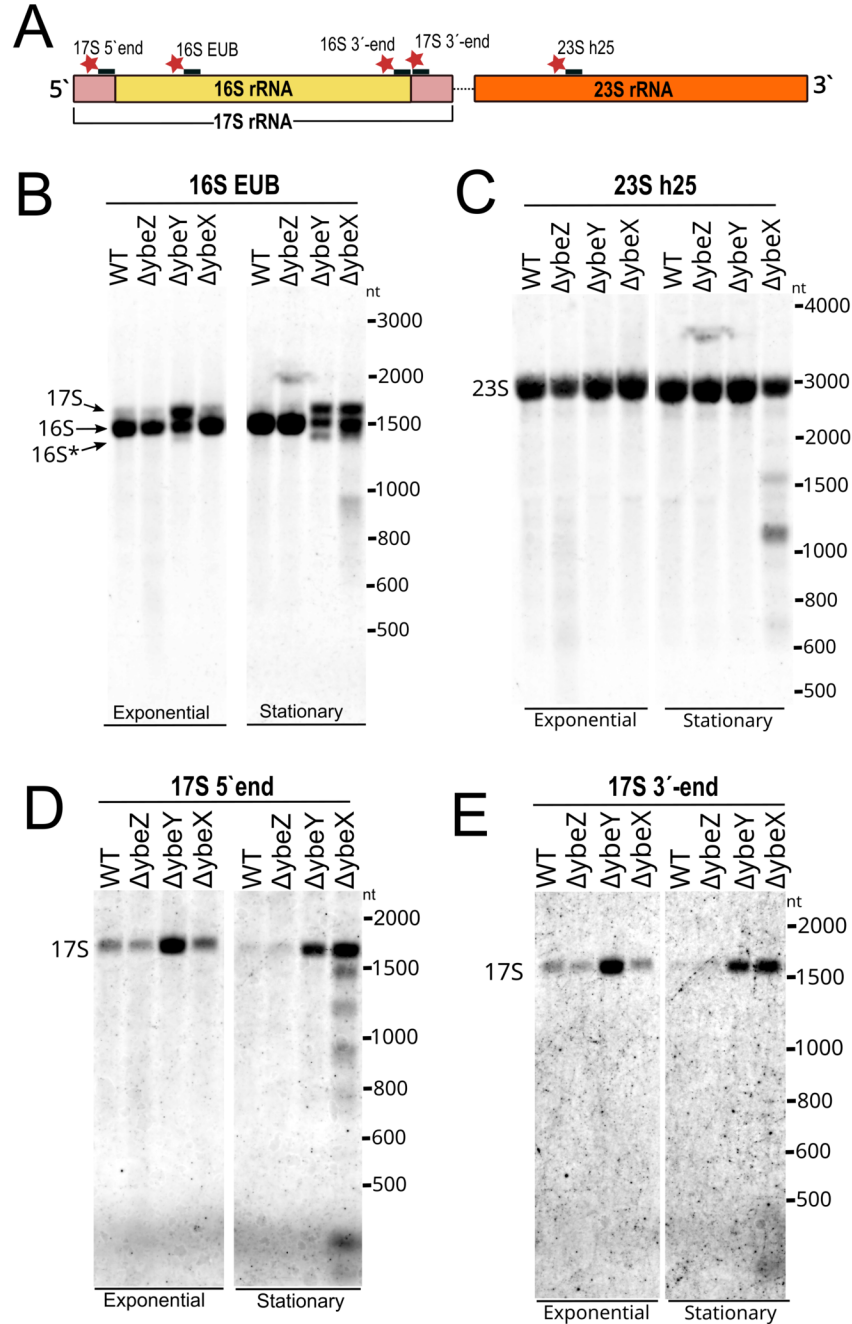
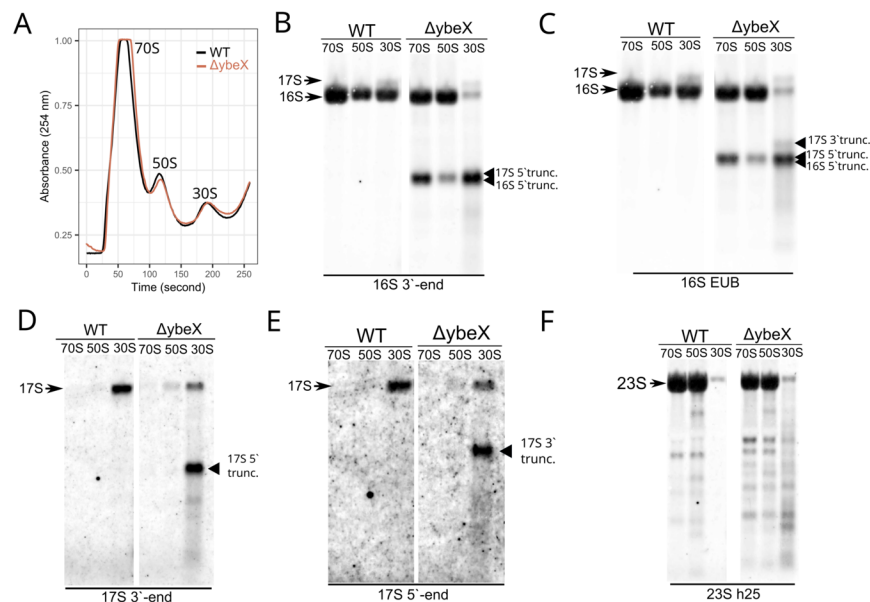
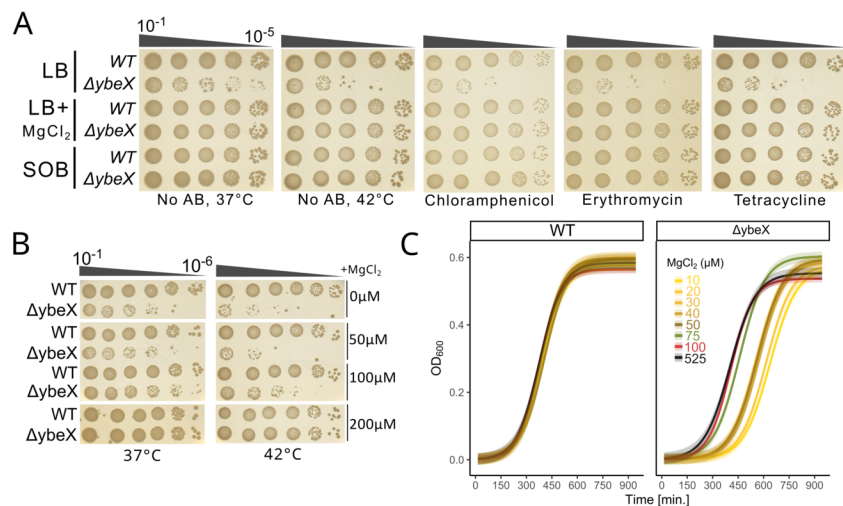


**Fig. 5. Deletion of *ybeX* leads to the accumulation of rRNA fragments during the stationary phase.** (A) rRNA operon scheme with locations of the Cy5-labelled oligonucleotides indicated as red stars. (B-E) Hot-phenol extracted total RNA samples from the exponential and stationary phase cultures of wild type,  $\Delta\psi\beta\epsilon\Psi$ ,  $\Delta\psi\beta\epsilon Z$ , and  $\Delta\psi\beta\epsilon E$  strains were separated on 1.5% denaturing agarose gel for Northern blotting. The cells were grown in LB medium at 37°C with aeration. The membrane was hybridized with 16S-EUB (B), 23S h25 (C), 17S 5'-end (D), and 17S 3'-end (E) rRNA targeting fluorescent oligos.

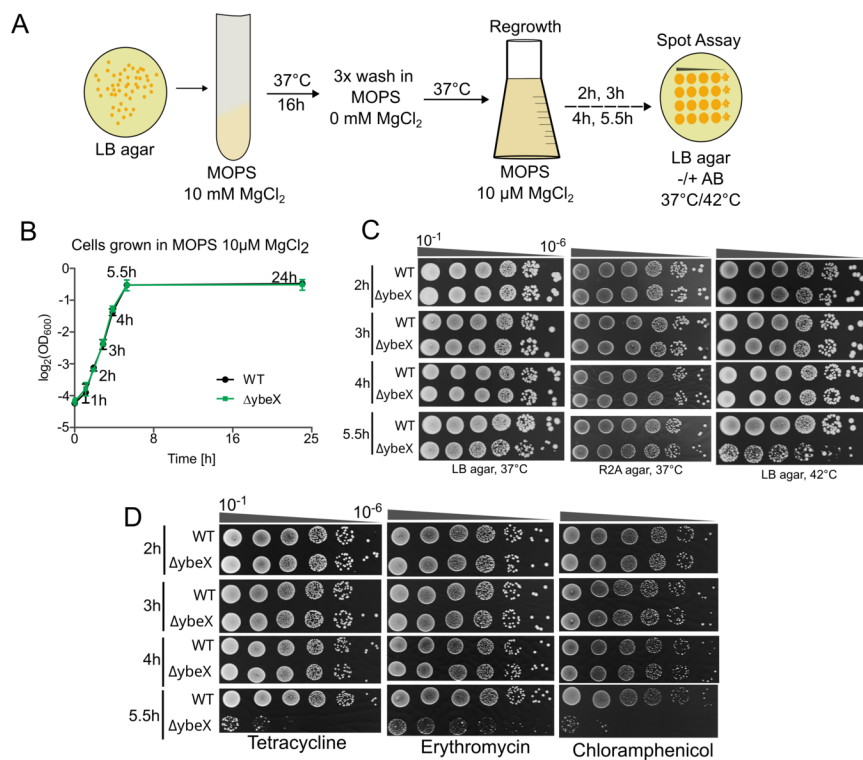


**Φιγ. 6.** Ριβοσομαλ φραξιονες οφ  $\Delta ybeX$  ζονταιν διστινξτ 16 $\Sigma$  ρPNA ανδ 17 $\Sigma$  πρε-ρPNA φραγμανξτ. (A) Sucrose gradient profiles of WT and  $\Delta ybeX$ . The strains were grown in LB medium at 37°C for 2 hours after the OD<sub>600</sub> reached 0.3. 10-30% sucrose gradients were used for sedimentation. The gradient profiles are representative of four independent experiments. (B-F) Northern blot hybridization of the same membrane using different Cy5-labelled oligonucleotides (see Table S3 and Fig. 5A). Truncated ribosomal RNA species are annotated as “trunc.”. The Cy5-labelled fluorescence oligonucleotides are 16S 3'-end, 16S (16S EUB), 17S 3'-end, 17S 5'-end, 23S (23S h25) specific, and each probe indicated under panels B-F.

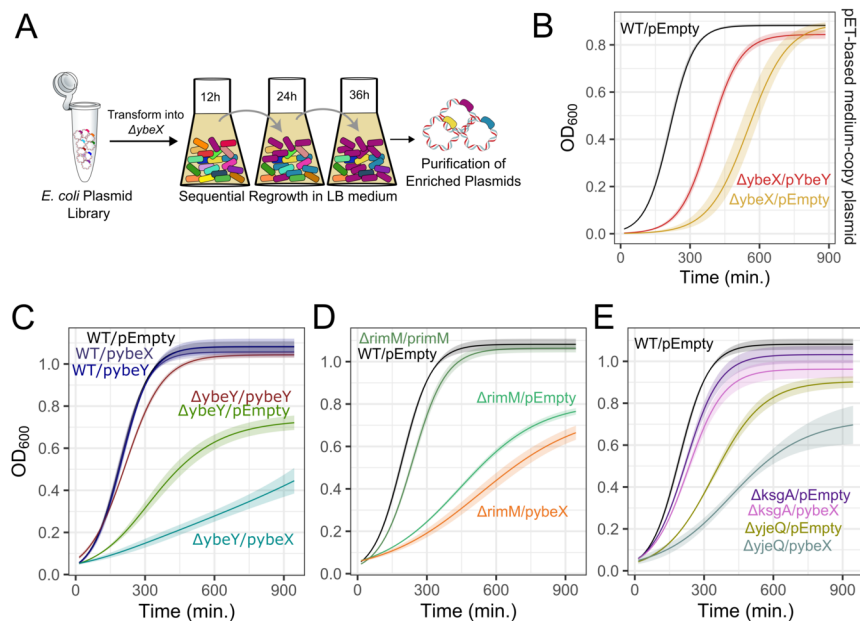


**Φιγ. 7.** Μαγνεσιουμ συπλεμεντατιον ρεξουεξ τξε  $\Delta ybeX$  πηνουτπξεξ ιν αριουξ γρωωτη μεδια. (A) The WT and  $\Delta ybeX$  cells were grown overnight in LB, SOB growth media, or LB supplemented with 10 mM MgCl<sub>2</sub>. The cells were serially diluted and spotted on LB agar plates. The plates with antibiotics were incubated at 37°C. There were also controls without antibiotics, denoted “No AB”, at 37°C or 42°C,

as indicated in the first two sub-panels. (B) A single colony of WT or  $\Delta\psi\beta\epsilon\Xi$  was grown overnight in the magnesium-limited peptide-based medium (PBM). 0  $\mu\text{M}$  denotes no  $\text{MgCl}_2$  supplementation; otherwise, PBM is supplemented with 50, 100 and 200  $\mu\text{M}$   $\text{MgCl}_2$ . The cells were plated as in panel A. (C) WT and  $\Delta\psi\beta\epsilon\Xi$  cells were grown overnight at 37°C in MOPS minimal medium supplemented with indicated concentrations of  $\text{MgCl}_2$  and 0.5% glucose. The outgrowth from these stationary phase cultures was tested in 1xMOPS minimal medium (0.5% glucose, 525  $\mu\text{M}$   $\text{MgCl}_2$ ) in 96-well plates at 37°C with aeration. The growth curves summarize three independent experiments shown as fitted logistic curves. Shaded areas represent the 95% CI-s.



**Φιγ. 8. Της γρωτη τρανσιτιον ιντο της στατιοναρψ πηασε λεαδς το της  $\Delta\psi\beta\epsilon\Xi$  πηενοτψπε.** (A) A scheme of the experimental setup is given. A single colony was inoculated into MOPS minimal medium supplemented with 10 mM  $\text{MgCl}_2$  and grown overnight at 37°C. The next day, saturated cultures were washed three times to remove residual magnesium and regrown in 10  $\mu\text{M}$   $\text{MgCl}_2$ -containing MOPS. Aliquots for plating on LB agar were taken at 2, 3, 4 and 5.5 hours. The LB agar plates either contained or did not contain antibiotics, as shown on panels D and E, and they were incubated overnight at 37°C or 42°C. (B) The growth of the wild-type and the  $\Delta\psi\beta\epsilon\Xi$  strains was monitored at an optical density of 600 nm in MOPS minimal medium supplemented with 10  $\mu\text{M}$   $\text{MgCl}_2$  and 0.5% glucose. The mean optical densities of three biological replicates are shown with 95% CI-s. (C) Dot spot experiments were conducted as in Fig. 7A, and the cells were collected from indicated time points, as in panel B. The  $\Delta\psi\beta\epsilon\Xi$  cells differed from wild-type in growth phenotype only when collected for the outgrowth spot assay at the 5.5h time point. (D) When the outgrowth spot assay plates contained tetracycline, erythromycin or chloramphenicol (at sub-MIC concentrations listed in Materials and Methods), severe growth inhibition was observed at the 5.5h time point.



**Φιγ. 9. ΨβεΨ οερεξπρεσσιον παρτιαλλψ ρεσσυεσ τησ δελαψεδ ουτγρωτη ιν $\Delta\psi\beta\epsilon\Xi$  μυταντ. (A)** A scheme of *E. coli* open reading frame plasmid library selection experiment for the search of compensatory plasmids rescuing the  $\Delta\psi\beta\epsilon\Xi$  extended lag phase phenotype. The selection involved sequential regrowth in 25 mL LB medium containing 50  $\mu\text{g}/\text{mL}$  Zeocin. Every 12 hours, a 1:100 culture sample was transferred to a fresh LB and incubated for another 12 hours at 37°C with aeration. **(B)** Overexpression of YbeY from a pET-based plasmid under the control of taq promoter in the presence of 1 mM IPTG leads to shortened growth lag in the  $\Delta\psi\beta\epsilon\Xi$  background. **(C)** YbeX overexpression from a single copy TransBac library plasmid in the presence of 1mM IPTG has a profound negative effect on the growth of the  $\Delta\psi\beta\epsilon\Xi$ . The wild-type and  $\Delta\psi\beta\epsilon\Xi$  strains were conjugated with the backbone TransBac library plasmid (empty), *ybeX* or *ybeY* overexpressing single-copy plasmids. The cells were grown in LB liquid medium with tetracycline and 1 mM IPTG. **(D-E)**  $\Delta rimM$  and  $\Delta\psi\theta\epsilon X$  Keio mutant strains were conjugated with the indicated TransBac library plasmids as in panel C. The outgrowth from stationary phase cultures was monitored with aeration in 96-well plates in LB medium at 37°C. The logistic curve fits summarize three to four biological replicates, each comprising a minimum of three technical replicates. Shaded areas represent 95% CI-s.